

masses and, therefore, is theoretically unhelpful (5). In this patient, however, gallium scintigraphy correctly diagnosed the coexistence of osteomyelitis by its discordance with the bone scan at known sites of leukemic infiltration. We would suggest the use of gallium scintigraphy or labeled white blood cells in this clinical setting.

The third and fourth patients illustrate the fact that leukemic infiltration can result in photopenic areas on bone scintigraphy. This is due to either compromise to the vascular supply to bone or to bone necrosis caused by the pressure effect from leukemic infiltration. The fourth patient had begun consolidation therapy including high doses of dexamethasone, which has reportedly been associated with avascular necrosis (6). The presence of focally increased uptake in the lumbar spine, metaphyseal abnormality in the femur and vertebral compression fracture, however, correctly indicated disease relapse. Photopenia on bone scintigraphy has been previously reported and may occur at presentation or at the time of relapse (7). Photopenia also has been described in relation to methotrexate therapy in the absence of leukemic infiltration (8). Leukemia is a rare cause of a focal photopenic lesion on bone scintigraphy but should be considered in the differential diagnosis, especially in the presence of concomitant abnormal uptake in the metaphyseal regions of the lower limbs and other focal bone scan abnormalities. A vertebral compression fracture developed at the time of disease relapse in the fourth patient. Alterations in mineral homeostasis and bone mass have been reported in patients with ALL both at the time of diagnosis and after treatment involving prednisone and methotrexate. Halton et al. (1) described defective mineralization as the mechanism for decreased bone mass. Therefore, patients with ALL can develop stress and compression fractures at the time of presentation or after treatment, which may be evident on scintigraphy. Alternatively, this complication may be due to a destructive process by leukemic cells. A review by Ribeiro et al. (4) described vertebral compression fractures in 1.6% of patients at the time of diagnosis. Vertebral compression fractures should be considered in the spectrum of potential scintigraphic abnormalities in patients with ALL.

In performing pediatric bone scans, special attention should be paid to correct technique to acquire precisely symmetrical images with the limbs as straight as possible so that the appearance of the epiphyseal-metaphyseal junction can be properly assessed. Lack of attention to technical detail may lead to diagnostic inaccuracy, because the growth plates may appear blurred if not imaged perpendicular to the collimator. There is usually a clear differentiation between the intense, symmetrical horizontal uptake in the growth plates and low-level uptake in the adjacent metaphyses. When there is a loss of distinction of the epiphyseal-metaphyseal junction and abnormal uptake in the metaphyseal regions, pathological processes such as leukemia, lymphoma, metastatic neuroblastoma or osteomyelitis should be considered, because all of these processes can cause symmetrical metaphyseal abnormalities. Radiographic examination of positive scintigraphic sites should be performed and correlated with scintigraphy.

CONCLUSION

Knowledge of scintigraphic changes that occur in the setting of acute childhood leukemia and its treatment will expedite the early diagnosis of leukemia at presentation and the diagnosis of complications during therapy.

REFERENCES

1. Halton J, Atkinson SA, Fraher L, Webber CE, Cockshott WP, Tam C. Mineral homeostasis and bone mass at diagnosis in children with acute lymphoblastic leukemia. *J Pediatr* 1995;126:557-564.
2. Clausen N, Gotze H, Pedersen A, Riis-Petersen J, Tjalve E. Skeletal scintigraphy and radiography at onset of acute lymphocytic leukemia in children. *Med Pediatr Oncol* 1983;11:291-296.
3. Masera G, Carnelli V, Ferrari M, Recchia Bellini F. Prognostic significance of radiological bone involvement in childhood acute lymphoblastic leukaemia. *Arch Dis Child* 1977;52:530-533.
4. Ribeiro RC, Pui C, Schell MJ. Vertebral compression fracture as a presenting feature of acute lymphoblastic leukemia in children. *Cancer* 1988;61:589-592.
5. Milder MS, Glick JH, Henderson ES, Johnston GS. Ga-67 scintigraphy in acute leukemia. *Cancer* 1973;32:803-808.
6. Chan-Lam D, Prentice AG, Copplestone JA, Weston M, Williams M, Hutton CW. Avascular necrosis of bone following intensified steroid therapy for acute lymphoblastic leukaemia and high grade malignant lymphoma. *Br J Haematol* 1994;86:227-230.
7. Morrison SC, Adler LP. Photopenic areas on bone scanning associated with childhood leukemia. *Clin Nucl Med* 1990;16:24-26.
8. Sty J, Babbitt D, Boedecker R. Bone scintigraphy: methotrexate associated bone necrosis. *Wis Med J* 1979;78:32-33.

Reverse Ventilation-Perfusion Mismatch in Lung Cancer Suggests Intrapulmonary Functional Shunting

Myriam Wartski, Eric Zerbib, Jean-François Regnard and Philippe Hervé

Departments of Nuclear Medicine, Thoracic Surgery and Respiratory Physiology, Marie Lannelongue Surgical Center, Le Plessis-Robinson, France

We report on a patient with squamous cell cancer of the left lung who was first considered ineligible for surgery because of severe hypoxemia. A ventilation-perfusion scan showed "reverse" ventilation-perfusion mismatch, with 20% of the total lung perfusion going to the left lung, which showed no ventilation with radioactive aerosols. This pattern suggested that the hypoxemia was due to intrapulmonary functional shunting and could therefore be improved by surgical resection of the tumor. Balloon occlusion of the left

pulmonary artery resulted in an immediate rise in PaO₂, indicating a right-to-left intrapulmonary shunt. After left pneumonectomy, PaO₂ levels were normal. This patient provides an example of dysregulation of the pulmonary hypoxic vasoconstriction response in a non-small cell lung cancer. Lung cancer patients with severe hypoxemia should undergo ventilation-perfusion scanning to look for reverse ventilation-perfusion mismatch suggestive of intrapulmonary functional shunting.

Key Words: bronchial cancer; hypoxemia; intrapulmonary functional shunting; ventilation-perfusion lung scan

J Nucl Med 1998; 39:1986-1989

Received Nov. 10, 1997; revision accepted Feb. 23, 1998.

For correspondence or reprints contact: Myriam Wartski, MD, Department of Nuclear Medicine, Marie Lannelongue Surgical Center, 133 Avenue de la Resistance, 92 350 Le Plessis-Robinson, France.

We report a case of intrapulmonary functional shunting in a patient with lung cancer and severe hypoxemia. Ventilation-perfusion lung scintigraphy showed reverse ventilation-perfusion mismatch suggestive of intrapulmonary functional shunting. PaO₂ levels returned to normal after left pneumonectomy.

CASE REPORT

A 68-yr-old man was admitted for surgery of a radiographically diagnosed tumor in the upper lobe of the left lung. CT showed a 4-cm mass. Bronchoscopy demonstrated complete obstruction of the upper and lower left bronchi by a tumor. Histological studies of the bronchial biopsy specimen established the diagnosis of squamous cell carcinoma. The patient was evaluated for surgical resection. Concurrent medical problems included non-insulin-dependent diabetes mellitus, moderate chronic bronchitis and systemic arterial hypertension treated for 10 yr with a beta-blocker (labetalol) and a calcium channel blocker (nifedipine). Spirometry showed decreases in forced expiratory volume in 1 sec (FEV₁) to 1.43 liter (57% of predicted), in forced vital capacity (FVC) to 2.13 liter (66% of predicted), in the FEV₁-to-FVC ratio to 67%, in total lung capacity to 5.63 liter (96% of predicted) and in diffusion of carbon monoxide to 5.6 mmol/kPa min (74% of predicted).

Arterial blood gas analysis on room air showed severe hypoxemia, with a PaO₂ of 6.25 kPa (47 mmHg), a PaCO₂ of 4.32 kPa (33 mmHg) and 90% oxygen saturation; the hematocrit was 44.9 and the hemoglobin level was 15.2 g. On 100% oxygen, PaO₂ was 11.27 kPa (84.7 mmHg), suggesting a true shunt. The shunt fraction calculated using the simplified shunt equation developed by Pontoppidan et al. (1) was 45%, with an alveolar-arterial oxygen pressure difference [P(A-a)O₂] of 50.8 mmHg.

Exercise testing on a bicycle ergometer showed severe abnormalities: maximum oxygen uptake (VO₂ max) was decreased to 13 ml/kg/min (60% of predicted) and maximum power was 45 W (35% of predicted). Arterial oxygen saturation (SaO₂) decreased from 86% to 77%, and PaO₂ decreased from 47 mmHg at rest to 40 mmHg at maximum exercise. The patient was originally considered ineligible for surgery because of the severe hypoxemia and exercise limitation (2). A perfusion lung scan (^{99m}Tc-labeled albumin macroaggregates) showed that left lung perfusion contributed to 20% of total lung perfusion but that the left lung was not ventilated (radioactive aerosol: ^{99m}Tc phytate) (Fig. 1). A ventilation scan showed no evidence of bronchial impaction. This reverse ventilation-perfusion mismatch with severe hypoxemia suggested intrapulmonary shunting. Right heart catheterization showed normal hemodynamic values. During selective balloon occlusion of the left pulmonary artery, pulmonary artery pressure remained unchanged, but PaO₂ improved immediately from 47 mmHg to 72 mmHg on room air and oxygen saturation rose from 90% to 96%. These findings demonstrated that intrapulmonary shunting was occurring and suggested that pneumonectomy would be successful in reversing the hypoxemia.

Left pneumonectomy was performed. The tumor was classified T2N2, Stage IIIA. No evidence of pulmonary artery involvement was seen intraoperatively. The postoperative course was uneventful. Arterial blood gas analysis on room air showed a dramatic improvement in PaO₂ from 6.25 kPa (47 mmHg) before surgery to 10.6 kPa (79.5 mmHg) after surgery, with a concomitant rise in SaO₂ from 90% to 96.5%. PaCO₂ remained normal. The 100% oxygen test was normal, with a PaO₂ of 73.5 kPa (552 mmHg), a PaCO₂ of 4.1 kPa (31 mmHg) and a P(A-a)O₂ of 20.7 mmHg. The patient was discharged with an appointment for mediastinal radiation therapy. He did not experience any side effects of radiation therapy, and 1 yr later he had no evidence of residual or recurrent disease, hypoxemia or respiratory insufficiency.

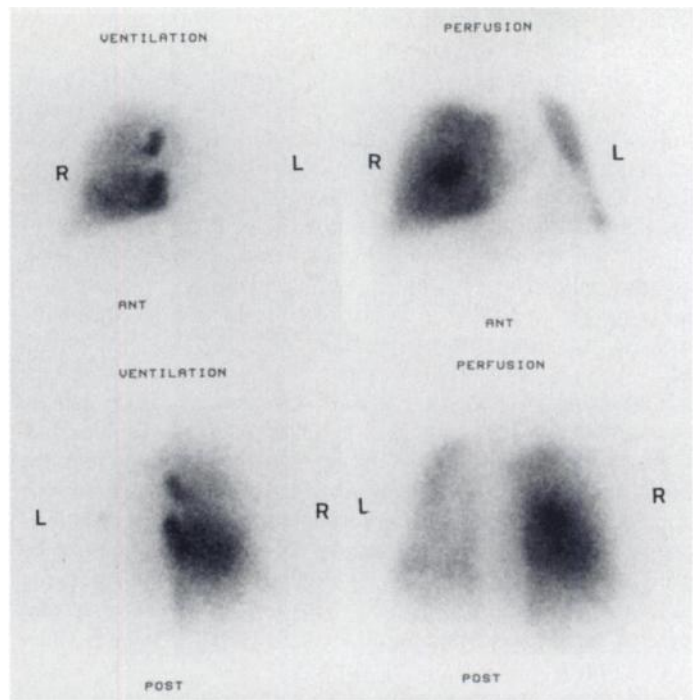


FIGURE 1. Ventilation and perfusion lung scans. Left lung was not ventilated but was partially perfused.

DISCUSSION

Several cases of reverse ventilation-perfusion mismatches, that is perfusion without ventilation, have been reported in the literature and are well founded physiologically. These situations correspond physiologically to blood shunted through poorly ventilated lung tissue and are, if extensive, of great physiologic importance, because blood shunted through poorly ventilated alveoli is a major cause of hypoxemia.

Causes of reverse ventilation/perfusion mismatch are as follows:

1. Bronchial obstruction (3-6): chronic obstructive pulmonary disease, mucus plugs or obliterative bronchiolitis.
2. Atelectasis associated with mechanical ventilation using positive pressure ventilatory support (7,8).
3. Pulmonary hypertension (primary and secondary) (9).
4. Pulmonary infection (10).
5. Lung carcinoma (11-14).

Other causes are uncommon and rare, including pulmonary embolism in the contralateral lung (15), metabolic alkalosis (16), pleural effusion (9), septic pulmonary emboli (17), transplanted lung (18), bronchopulmonary dysplasia (19) and congestive heart failure (20).

Surgical resection is the therapeutic approach most likely to cure lung carcinoma but is contraindicated in patients with severe hypoxemia. In proximal bronchial carcinoma, the non-ventilated lung is usually not perfused because the tumor commonly obstructs the pulmonary artery or because reflex hypoxic pulmonary vasoconstriction develops in response to the hypoventilation caused by the bronchial obstruction. Normally, in a case of regional pulmonary hypoxia caused by hypoventilation, perfusion tends to be redistributed to other, well-oxygenated ventilation regions because pulmonary arterioles are the site of vasoconstriction and ventilation-perfusion match is usually observed. This hypoxic pulmonary vasoconstriction

response has an established role in preserving the ventilation-perfusion balance. It is one of the major factors responsible for maintaining pulmonary blood flow to well-ventilated alveoli and, therefore, for maintaining PaO₂ values within normal ranges by redistributing the pulmonary blood flow to normoxic ventilatory units by means of vessel recruitment. This phenomenon may serve as an autoregulatory mechanism that adjusts regional ventilation-perfusion ratios by local autoregulation or through the action of the autonomic nervous system (21). It is still the only known vascular feedback control mechanism in the lung. This mechanism is also used to interpret ventilation-perfusion mismatch observed in certain cases of pulmonary embolism.

In proximal bronchial carcinoma, alveolar hypoxia is usually followed by a normal hypoxic arterial constrictive response that decreases or abolishes pulmonary perfusion. In this patient, the left bronchus was completely obstructed by lung carcinoma. But, contrary to the concept described here, reverse ventilation-perfusion mismatch was observed. The ventilation-perfusion scan pattern was typical of dysregulation of reflex hypoxic pulmonary arterial constriction. The left bronchus was completely obstructed, whereas no evidence of pulmonary artery obstruction was found during surgery.

If the hypoxic arterial response is impaired, the unventilated alveoli continue to receive their blood supply and, as a result, shunting, i.e., intrapulmonary functional shunting (IFS) and thus hypoxemia develop. This shunt is located into the lung and is not anatomical but functional because it concerns the admixture of shunted, nonventilated hypoxic, blood flow into the pulmonary vascular bed. We did not observe macroaggregates (MAA) of human albumin labeled with ^{99m}Tc localized in extrapulmonary organs such as in the kidneys, brain or spleen. Indeed, the mechanism of IFS is different from, for example, anatomical intrapulmonary shunts observed in liver cirrhosis (22) or in pulmonary arteriovenous fistulae (23). For example, in cirrhosis and hepatitis (22), true shunting through arteriovenous anastomoses associated with dilatation of precapillary vessels had been proposed as a mechanism for the development of right-to-left shunt. In this patient with true right-to-left shunt, activity may be seen in the systemic circulation when ^{99m}Tc-MAA is injected intravenously. In this case report, the dysregulation of the physiological mechanism results in an increase in the alveolar-arterial oxygen pressure difference and, therefore, in arterial hypoxemia. Surgical resection of the nonventilated lung in this patient removed the site of IFS and, as a result, corrected the hypoxemia.

The exact mechanism of dysregulation of hypoxic pulmonary vasoconstriction in this patient is not clear. Development of intratumoral blood neovessels or production of vasodilating substances by the tumor are reasonable hypotheses. In this patient, there was no evidence of anemia or respiratory alkalosis, two factors known to inhibit hypoxic vasoconstriction in experimental models (16). The patient had been treated with nifedipine for 10 yr for moderate systemic arterial hypertension and was receiving this therapy at the time of the ventilation-perfusion scan.

Calcium channel blockers may explain the dysregulation of hypoxic vasoconstriction in this patient. Nifedipine is a powerful vasodilating agent of systemic vessels, it increases cardiac output in both normal subjects and cardiac patients. Simonneau et al. (24) showed that nifedipine acutely dilates pulmonary vessels constricted by hypoxia in patients with chronic airflow obstruction and acute respiratory failure. Experiments in isolated rat lungs have suggested that the calcium antagonist verapamil inhibits hypoxic pulmonary vasoconstriction (25).

Nifedipine relaxes the pulmonary artery of neonatal piglets and inhibits noradrenaline-induced contractions (26). Sakr and Mikkelsen (27) studied the physiological effects of the calcium-blocker nifedipine in isolated human pulmonary vessels. Specimens of macroscopically normal pulmonary vessels were obtained from patients undergoing surgery for lung tumors and were carefully dissected. Results suggest that nifedipine, by blocking the entry of extracellular calcium, inhibits potassium-induced contractions in isolated pulmonary vessels. Besides, nifedipine inhibits the activity of secretory cells (28). All these studies confirm that acute hypoxic pulmonary vasoconstriction depends on the availability of calcium to smooth muscle cells of the pulmonary arterial wall cells. In vivo studies confirm that nifedipine inhibits hypoxic pulmonary vasoconstriction during rest and exercise in patients with chronic obstructive pulmonary disease (29). Precisely, FEV₁ was decreased in this patient with squamous cell carcinoma that resulted in airway obstruction. We strongly suspect that the calcium channel blocker was the promoting factor in the lack of hypoxic vasoconstriction and, as a result, the explanation for the severe hypoxemia in this patient.

The changes produced by balloon occlusion of the left pulmonary artery established that IFS was the cause of hypoxemia of this patient: arterial saturation rose, whereas pulmonary artery pressure remained unchanged during the procedure. These findings led to the decision to remove the tumor.

Hypoxemia seems to be caused by IFS in a small proportion of lung cancer patients without severe chronic obstructive pulmonary disease. In those patients, IFS usually disappears after surgical resection of the lung harboring the tumor. Reverse ventilation-perfusion mismatch has been reported in lung cancer patients (11-14), although we are not aware of previous cases in which both ventilation-perfusion scanning and right heart catheterization were performed and in which an increase in PaO₂ levels with no change in pulmonary artery pressure were found during occlusion of the pulmonary artery. Right heart catheterization is useful in this context for predicting the effect of surgery on the hypoxemia. The most noteworthy finding of this case report is that the hypoxemia was corrected by pneumonectomy. PaO₂ before surgery was 47 mmHg, 72 mmHg during balloon occlusion of the left pulmonary artery and 79.5 mmHg after surgery.

Severe hypoxemia is usually a contraindication to surgery for lung cancer. In lung cancer patients, lung resection offers the best hope for long-term survival. However, removal of lung tissue can impair postoperative ventilatory function in patients with chronic airflow limitation and hypoxemia, which can lead to cardiopulmonary complications, some of which can be fatal. Quantitative lung scanning can predict the lung function loss that will result from the surgical procedure and is therefore helpful in determining those patients in whom the surgical risk is acceptable. In most studies, ventilation versus perfusion scanning offered comparable accuracy for preoperative lung function evaluation (30,31). In our institution, perfusion lung scanning is the preferred technique. In some patients, however, most notably those with severe hypoxemia, both perfusion and ventilation lung scanning should be performed to look for reverse ventilation-perfusion mismatch indicative of intrapulmonary functional shunting.

CONCLUSION

Intrapulmonary shunting should be looked for in lung cancer patients with severe hypoxemia not explained by pulmonary volume or function limitation. Ventilation-perfusion scanning shows reverse ventilation-perfusion mismatch. A rise in PaO₂

levels during occlusion of the pulmonary artery confirms the diagnosis. Hypoxemia resolves after pneumonectomy. Intratumoral functional shunting should be recognized so that the patient can benefit from surgical treatment.

REFERENCES

1. Pontoppidan H, Geffin B, Lowenstein E. Acute respiratory failure in adults. *N Engl J Med* 1972;287:743-51.
2. Richter Larsen K, Svendsen UG, Milman N, Brenoe J, Petersen BN. Exercise testing in the preoperative evaluation of patients with bronchogenic carcinoma. *Eur Resp J* 1997;10:1559-1565.
3. Carvalho P, Lavender JP. The incidence and etiology of the ventilation-perfusion reverse mismatch defect. *Clin Nucl Med* 1989;14:571-576.
4. Fuentes RT, Holmes RA. Reverse radioaerosol/radioperfusion distribution in pulmonary endobronchial obstruction. *Clin Nucl Med* 1990;15:217-221.
5. Cunningham DA, Lavender JP. Krypton 81m ventilation scanning in chronic obstructive airway disease. *Br J Radiol* 1981;54:110-116.
6. Kao CH. Reverse ventilation/perfusion mismatch. *Semin Nucl Med* 1997;27:183-185.
7. Hawker FH, Torzillo PJ, Southee AE. PEEP and "reverse mismatch." A case where less PEEP is best. *Chest* 1991;99:1034-1036.
8. Kim CK, Heyman S. Ventilation/perfusion mismatch caused by positive pressure ventilatory support. *J Nucl Med* 1989;30:1268-1270.
9. Engeler CE, Kuni CC, Tashjian JH. Regional alterations in lung ventilation in end-stage primary pulmonary hypertension: correlation between CT and scintigraphy. *AJR* 1995;164:831-835.
10. Li DJ, Stewart I, Miles KA, et al. Scintigraphic appearance in patients with pulmonary infection and lung scintigrams of pulmonary embolism. *Clin Nucl Med* 1994;19:1091-1093.
11. Watanabe N, Hirano T, Inoue T, et al. Transient unilateral reverse ventilation/perfusion mismatch in a patient with lung cancer. *Clin Nucl Med* 1992;17:705-708.
12. Shih WJ, Jonston EH, Jonston HW. Reversed abnormal ventilation perfusion scintigraphy in endobronchial squamous cell carcinoma. *Eur J Nucl Med* 1982;7:523-525.
13. Gherty KG, Dick C, McGovern J, Conroy RM, Mahutte CK. Refractory hypoxemia due to intrapulmonary shunting associated with bronchioalveolar carcinoma. *Chest* 1997;111:1120-1121.
14. Shih WJ, Dillon ML. Matched ventilation-perfusion becomes mismatched ventilation-perfusion lung imaging after resolution of carcinoma of the bronchus. *Clin Nucl Med* 1994;19:279-286.
15. Armas R. Large reverse mismatch associated with pulmonary embolism. *Clin Nucl Med* 1994;19:910-925.
16. Benumof JL, Wahrenbrock EA. Blunted hypoxic pulmonary vasoconstriction by increased lung vascular pressures. *J Appl Physiol* 1975;38:846-850.
17. Spencer RP. Ventilation/perfusion reverse mismatch in septic pulmonary emboli. *Clin Nucl Med* 1996;21:328-329.
18. Kuni CC, Ducret RP, Nakhleh RE, Boudreau RJ. Reverse mismatch between perfusion and aerosol ventilation in transplanted lungs. *Clin Nucl Med* 1993;18:313-317.
19. Slavin JD Jr, Mathews J, Spencer RP. Pulmonary ventilation-perfusion and reverse mismatches in infant. *Clin Nucl Med* 1985;10:708-709.
20. Zucker I, Heyman S, Ozdemir S. Reversed ventilation-perfusion mismatch involving a pediatric patient in congestive heart failure. *J Nucl Med* 1997;38:1681-1683.
21. Sostman HD, Neumann RD, Gottschalk A, Greenspan RH. Perfusion of non ventilated lung: failure of hypoxic vasoconstriction? *AJR* 1983;141:151-156.
22. Levin DP, Pison CF, Brandt M, et al. Reversal of intrapulmonary shunting in cirrhosis after liver transplantation demonstrated by perfusion lung scan. *J Nucl Med* 1991;32:862-864.
23. Suga K, Kuramitsu T, Yoshimizu T, Nakanishi T, Yamada N, Utsmi H. Scintigraphic analysis of hemodynamics in a patient with a single large pulmonary arteriovenous fistula. *Clin Nucl Med* 1992;17:110-113.
24. Simonneau G, Escourou P, Duroux P, Lockart A. Inhibition of hypoxic pulmonary vasoconstriction by nifedipine. *N Engl J Med* 1981;304:1582-1585.
25. McMurtry IF, Davidson AB, Reeves JT, Grover RF. Inhibition of hypoxic pulmonary vasoconstriction by calcium antagonists in isolated rat lungs. *Circ Res* 1976;38:99-104.
26. Perez-Vizcaino F, Villamor E, Moro M, Tamargo J. Pulmonary versus systemic effects of vasodilator drugs: an in vitro study in isolated intrapulmonary and mesenteric arteries of neonatal piglets. *Eur J Pharmacol* 1996;314:91-98.
27. Sakr M, Mikkelsen E. Effects of nifedipine on isolated human pulmonary vessels. *Gen Pharmacol* 1983;14:115-116.
28. Malaisse WJ, Boschero AC. Calcium antagonist and islet function. XI. Effect of nifedipine. *Horm Res* 1977;8:203-209.
29. Kennedy TP, Huang M Jr, Kallman CH, Zahka K, Schlott W, Summer W. Nifedipine inhibits hypoxic pulmonary vasoconstriction during rest and exercise in patients with chronic obstructive pulmonary disease. A controlled double-blind study. *Am Rev Respir Dis* 1984;129:544-551.
30. Wernly JA, DeMeester TR, Kircner PT, Myerowitz PD, Oxford DE, Golomb HM. Clinical value of quantitative ventilation-perfusion lung scans in the surgical management of bronchogenic carcinoma. *J Thorac Cardiovasc Surg* 1980;80:535-543.
31. Markos J, Mullan BP, Hillman DR, et al. Preoperative assessment as a predictor of mortality and morbidity after lung resection. *Am Rev Respir Dis* 1989;13:902-910.

Radiation Absorbed Doses to the Walls of Hollow Organs

James B. Stubbs, Jeffrey F. Evans and Michael G. Stabin

NCO Cath, Inc., Roswell, Georgia; Nuclear Engineering Program, Ohio State University, Columbus, Ohio; and Oak Ridge Institute for Science and Education, Oak Ridge, Tennessee

Many radiopharmaceuticals are excreted from the body through the gastrointestinal (GI) tract. The doses to the walls of the organs involved often are very significant. As significant fractions of the administered activity pass through them, these organs may receive the highest doses in the body for many radiopharmaceuticals. The absorbed dose to these walled organs, from activity in their contents, is typically calculated as 50% of the average absorbed dose to the contents, for nonpenetrating emissions. The internal surface of the GI tract, and to a certain extent the urinary bladder, is lined with a variable thickness of mucus. In addition, the radiosensitive cell populations (crypt or stem cells) are located at some depth into the mucosa. These two factors suggest that the surface dose, often used to characterize the clinically relevant absorbed doses for walled organs, may represent an overestimate in some cases. **Methods:** In this study, the radiation transport code MCNP was used to simulate the deposition of energy from nonpenetrating

emissions of several radionuclides of interest: ^{90}Y , $^{99\text{m}}\text{Tc}$, ^{123}I and ^{131}I . Absorbed doses as a function of distance from the wall-contents interface were calculated for three geometric shapes representing different organs along the routes of excretion. **Results:** The absorbed dose from nonpenetrating emissions to the sensitive cell populations was consistently lower than estimated by the standard model assumption. The simulated absorbed doses to radiosensitive cells in the GI tract for $^{99\text{m}}\text{Tc}$ and ^{123}I are tenfold lower; those for ^{131}I are fivefold lower and those for ^{90}Y are 20% lower. **Conclusion:** This study demonstrates that the normally reported dose to the walls of hollow organs probably should be modified to account for the attenuation of these nonpenetrating emissions in the linings of the walls. This study also demonstrates that Monte Carlo codes continue to be useful in the evaluation of the dose to sensitive cells in walled organs.

Key Words: Monte Carlo; radiation absorbed doses; gastrointestinal tract; electrons; beta particles

J Nucl Med 1998; 39:1989-1995

Received Nov. 20, 1997; revision accepted Feb. 25, 1998.

For correspondence or reprints contact: Michael G. Stabin, PhD, Radiation Internal Dose Information Center, Oak Ridge Institute for Science and Education, P.O. Box 117, Oak Ridge, TN 37831-0117.